*Reprinted from the preprint volume of the **10th Co** **on Satellite Meteorology and Oceanography**, 9–1 2000, Long Beach, CA, by the AMS, Boston, MA.*

P2.19 MODELING DIRECT IRRADIANCE FROM GOES VISIBLE CHANNEL USING GENERALIZED CLOUD INDICES.

Pierre Ineichen
University of Geneva, Switzerland

Richard Perez* and Marek Kmiecik,
ASRC, Albany, New York

David Renné,
NREL, Golden, Colorado

1. INTRODUCTION

Simple operational models predicting global irradiance from the visible channel of geostationary satellites are based on the observation that the relationship between planetary albedo [i.e., normalized satellite count] and atmospheric transmissivity [i.e., normalized global irradiance] is linear (Schmetz, 1989).

Direct, diffuse irradiance and other solar radiation components are generally derived as a byproduct of global irradiance using transposition models, many of which have been developed for solar energy applications. The compounding of models reduces achievable precision.

Ineichen and Perez (1999) recently introduced a one-step approach to model other solar components directly from the satellite counts This paper presents an initial validation of this one-step model against high quality hourly ground measurements in Albany, NY, covering a 9-month period. Results are compared to the traditional approach of compounding two models to derive direct and diffuse irradiance. The paper also investigates how readily, or potentially, available ancillary information (e.g., cloud cover from the National Weather Service) could lead to operational performance improvements.

2. METHODS

2.1 Traditional vs. One-Step Model

Traditional Approach: The linear planetary albedo-transmissivity relationship (Schmetz, 1989) is at the basis of many operational models, including the Heliosat method (Moussu et al., 1989) and its recent derivatives (Hammer et al., 1998, Zelenka et al., 1999). The governing equation of this type of model is:

$$G / Ghk = (1-n) + \varepsilon \qquad (1)$$

where G is the global irradiance, Ghk is the clear sky global irradiance obtained from a model adjustable for broad-band (Linke) turbidity and ground elevation (e.g., Kasten, 1984), n is a ***cloud index***, and ε is a residual value of the ratio G/Ghk corresponding to heavily overcast conditions (n=1). The cloud index n is obtained from:

$$n = (C - Cmin) / (Cmax - Cmin) \qquad (2)$$

where C, Cmin, and Cmax are the current, the minimum possible and the maximum possible satellite pixel counts normalized for sun-earth distance, solar zenith angle as well as secondary air mass and backscattering effects (e.g., see Ineichen & Perez., 1999), so as to be representative of planetary albedo.

Operationally, the (Cmax - Cmin) factor represents the model's ***dynamic range.*** This may be fixed (e.g., from the satellite's calibration), however it is considered more efficient to keep track of the dynamic range through a time-evolving window, thereby accounting for local ground albedo variations and eliminating the need for a determination of the satellite sensor's calibration.

Direct and diffuse irradiances are extrapolated from global irradiance. In this study, the Dirint (modified DISC) model (Perez et al., 1992) is used for this purpose.

One Step Approach: The difficulty of deriving a totally solar geometry-independent cloud index led to the development of a generalized cloud index-based approach that would not need to be linearly related to the considered irradiance index (Ineichen & Perez, 1999). Indeed, observations of data from Goes and Meteosat against measurements in Albany and Geneva showed that the relationship between the cloud index and the global irradiance index tended to be slightly non-linear. However, the usefulness of the generalized cloud index concept becomes apparent when dealing with the prediction of components other than global irradiance, such as direct or diffuse, because the relationship of these components' indices against the cloud index is highly non-linear.

The governing equation of the one step model is,

$$X / Ghk = F_x(n, z) \qquad (3)$$

where X is the selected solar component impinging on a horizontal surface (e.g., direct horizontal irradiance) F_x is a function of the cloud index, n, and the solar zenith angle, z. Figure 1 shows one such experimentally-derived function for direct irradiance, established empirically from the Meteosat satellite and multi-site ground data (Ineichen & Perez, 1999).

2.2 Experimental Data

Ground data: Quality-controlled hourly measurements of global, direct and diffuse irradiance from Albany, New York, covering four seasons in 1995-1996 and three seasons in 1997-1998, were used for this analysis. Both sets of data were used to derive the one-step relationships between cloud index and the global, direct and diffuse indices. Validations were performed against the 1997-1998 data, both for the one-step and the classical models.

* *Corresponding author address*: Richard Perez, ASRC, 251 Fuller Rd., Albany, NY, 12203, email: perez@asrc.cestm.albany.edu

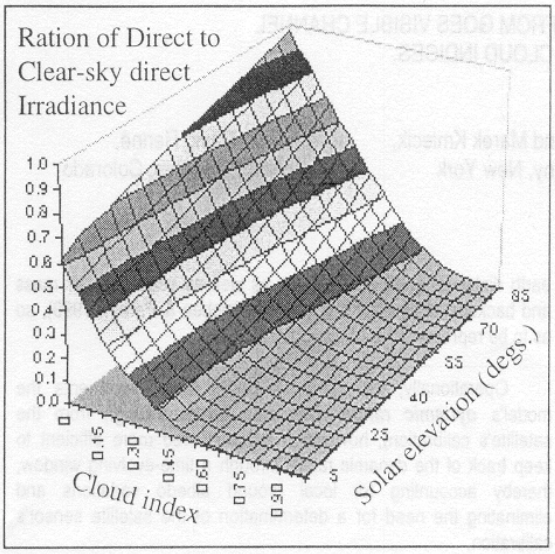

Figure 1: One-step relationship between the direct irradiance index, the satellite-derived cloud index and solar geometry

Satellite data: Image pixels closest to the Albany station covering a period from June 1995 to February 1999 were used for the analysis. The pixel resolution is 0.1-degree latitude by 0.1-degree longitude (obtained via sub-sampling and gridding of primary images). Data that did not overlap with ground measurement periods were used to observe the long-term variability of the dynamic range. In this process we noted that the calibration of GOES 8 had drifted substantially over time. This calibration drift is not a problem for the traditional model since this is capable of keeping track of the dynamic ranges' evolution over time and works in a relative context. However, the one step models do not have this capability yet. It was therefore critical to notice, and to account for the calibration drift in deriving these models.

2.3 Model Development for Testing

Traditional model: Five versions were prepared for this investigation.

- Version 1 is the model in its most primitive form with a fixed dynamic range and a constant Linke turbidity for the Kasten's clear sky model.
- Version 2 uses a time-evolving dynamic range for each ground pixel. The dynamic range is based on pixels recorded during an 18-day moving window, except in winter when the window is reduced to 10 days in order to account for rapid ground snow cover variations.
- Version 3 is the same as version 2, but with seasonal Linke turbidity adjustments based on several years of ground observation in Albany (Ineichen & Perez, 1999)
- Version 4 is similar to version 3 but refines the dynamic range-tracking algorithm by adding available external information. Indeed the shorter winter window, although adequate to pick up fast evolving ground albedos, could lead to erroneous results at times of prolonged cloudiness, overestimating the dynamic range's lower bound, hence overpredicting irradiance. Using external information readily available from the National Weather Service -- cloud cover -- we modified the algorithm to only allow pixels corresponding to a "clear sky" signal from the closest National Weather Service site into the calculation of the current's dynamic range's lower bound.
- Version 5 is similar to version 4, but uses additional external information: measured current regional Linke turbidity replaces the seasonal look-up table -- regional turbidity is estimated from direct irradiance measurements in Albany. The turbidity corresponding to the pixels used to define the lower bound of the dynamic range is used in the Kasten's clear sky model.

One Step Model: Three models were derived for global, direct and diffuse irradiance respectively: A 3-D envelope, function of the cloud index, n, and of the solar zenith angle was empirically generated for each component, based on 1995-98 ground and satellite data.

3. MODEL PERFORMANCE ASSESSMENT

The benchmarks of performance assessment include (1) Root mean square mean bias errors (resp. RMSE and MBE); (2) Effective accuracy; (3) Frequency distribution comparison between measured and modeled components

3.1 RMSE and MBE

The RMSE and MBE for each model and each season analyzed are reported, in both absolute (W/sq.m) and relative terms, in Table 1.

Traditional model: The largest gain in performance occurs when going from a fixed default ground albedo (dynamic range's lower bound) to a localized time-evolving albedo. The default, based on a regional estimate, was too low and forced the model to underestimate global irradiance. The calculation of direct from global compounds this underestimation. Version 1's shortcoming is particularly felt in winter, when the ground albedo may at times be high due to snow cover. Version 3, using a seasonal turbidity average, leads to minor improvements in the spring and fall, but to degradation in winter, particularly visible for the direct component. This is an result of the short winter albedo tracking window that may at times raise the dynamic range's lower bound too high during periods of extended cloud cover. Version 2 tended to mitigate this problem by using a conservative clear sky turbidity, while version 3 appropriately applies a low wintertime turbidity. By using external information to handle the albedo tracking, version 4 tends to correct this problem, leading to a satisfactory performance in the spring and fall and some noticeable improvement in winter. Version 5 links the albedo tracking procedure with a read on the regional turbidity, hence leads to a more uniform season-to-season performance.

One-step model: This model still uses a fixed dynamic range, but the dynamic range's lower bound was optimized for the Albany pixel using the long-term satellite data stream. The Linke turbidity used for the global and direct clear sky model is a seasonally fitted envelope. The performance of this model is remarkable, approaching version 4 for global and diffuse, and approaching version 5 for direct without the benefit of any external input. Hence, the one-step pixel-to-direct non-linear relationship appears to be a better alternative than the compounding of two models.

TABLE 1

				Traditional					One	Traditional					One
	average			V-1	V-2	V-3	V-4	V-5	Step	V-1	V-2	V-3	V-4	V-5	Step
				Absolute errors						Relative errors					
Global															
	fall 97	246	MBE	-35	-24	3	-3	-8	0	-14%	-10%	1%	-1%	-3%	0%
	winter 97-8	185		-51	-4	22	9	-7	-5	-28%	-2%	12%	5%	-4%	-3%
	spring 98	376		-23	-22	-10	-9	-11	8	-6%	-6%	-3%	-2%	-3%	2%
	ALL	**269**		**-36**	**-17**	**5**	**-1**	**-9**	**1**	**-14%**	**-6%**	**2%**	**0%**	**-3%**	**0%**
	fall 97		RMSE	67	61	61	58	58	56	27%	25%	25%	24%	24%	23%
	winter 97-8			84	65	78	61	57	71	45%	35%	42%	33%	31%	38%
	spring 98			68	67	64	64	64	65	18%	18%	17%	17%	17%	17%
	ALL			**73**	**64**	**68**	**61**	**60**	**64**	**27%**	**24%**	**25%**	**23%**	**22%**	**24%**
Direct															
	fall 97	311	MBE	-75	-60	40	21	3	18	-24%	-19%	13%	7%	1%	6%
	winter 97-8	177		-105	-4	84	54	10	-26	-59%	-2%	47%	31%	6%	-15%
	spring 98	336		-23	-30	5	6	1	-11	-7%	-9%	1%	2%	0%	-3%
	ALL	**278**		**-68**	**-31**	**43**	**27**	**5**	**-6**	**-24%**	**-11%**	**15%**	**10%**	**2%**	**-2%**
	fall 97		RMSE	168	161	167	141	142	143	54%	51%	53%	45%	45%	46%
	winter 97-8			237	155	208	170	144	154	134%	88%	118%	96%	81%	87%
	spring 98			110	114	110	112	112	112	33%	34%	33%	33%	33%	33%
	ALL			**172**	**143**	**162**	**141**	**133**	**138**	**62%**	**52%**	**58%**	**51%**	**48%**	**50%**
Diffuse															
	fall 97	100	MBE	-1	0	-8	-7	-4	-10	-1%	0%	-8%	-7%	-4%	-10%
	winter 97-8	99		-2	-1	-4	-5	-6	8	-2%	-1%	-4%	-5%	-6%	8%
	spring 98	145		1	7	1	1	1	-15	1%	5%	1%	1%	1%	-10%
	ALL	**115**		**-1**	**2**	**-4**	**-4**	**-3**	**-6**	**-1%**	**2%**	**-3%**	**-3%**	**-3%**	**-5%**
	fall 97		RMSE	50	51	50	47	44	48	51%	52%	51%	47%	44%	48%
	winter 97-8			65	43	48	47	48	51	66%	43%	48%	47%	48%	52%
	spring 98			53	52	50	50	50	55	37%	36%	34%	34%	34%	38%
	ALL			**56**	**49**	**49**	**48**	**47**	**52**	**49%**	**42%**	**43%**	**42%**	**41%**	**45%**

3.2 Effective Accuracy

The authors and colleagues recently introduced the notion of effective accuracy (Zelenka et al., 1999) that should complement any RMSE/MBE-based assessment. Because the comparison between ground and satellite involves an instantaneous pixel extended in space and a point measurement extended in time (via hourly integration), the best possible hourly RMSE achievable is only of the order of 10-15% (Zelenka et al., 1999). A measure of this natural discrepancy is the nugget effect of a variogram derived from ground measurements (Fig. 2). Accounting for this, the effective, intrinsic, accuracy of global prediction has been estimated at about 13%, and not 23% as benchmarked through the RMSE. Another measure of effective accuracy is the break-even distance from a measurement point beyond which the satellite becomes the most accurate source of time/site specific global irradiance. For global irradiance, this effective accuracy is estimated at 25 km.

For the direct component, while mean bias errors are satisfactory, RMSEs are considerably higher than for global -- averaging 50% in the best case. However this RMSE must also be discussed in an effective accuracy context, and for direct irradiance, the best possible achievable accuracy is considerably higher than for global. With current level of performance, the breakeven distance for direct is of the order of 45 km, down from 100 km with the version 1 traditional model.

3.3 Frequency Distributions

MBEs and RMSEs are measures of long term and short-term model performance relevant to overall and time site-specific concerns respectively. Frequency distributions bring a climatological dimension to model performance assessment that is particularly relevant to solar system design and operation, particularly when these systems are threshold-sensitive.

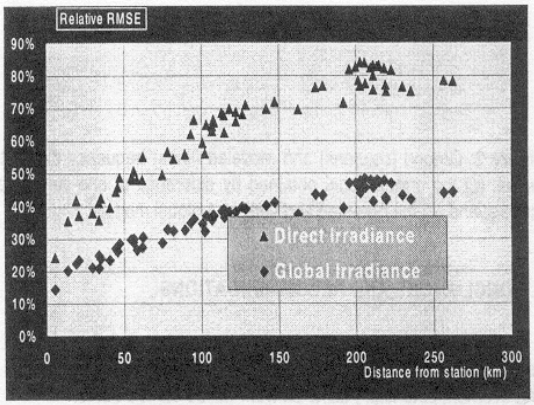

Figure 2: Degradation of hourly RMS accuracy as a function of Distance from a measuring station

Figure 3 shows the ground and modeled distributions for the one-step direct model (a), the version 1 traditional direct model (b), the direct model obtained by difference of one-step global and one-step diffuse models (c), the one-step and version 1 diffuse models (d), and the one-step and version 1 global models (e). The ground-based frequency distributions are displayed as columns, while the satellite distributions are displayed as lines.

The improvement from the classical model version to the one-step is considerable. This improvement is particularly noticeable for direct.

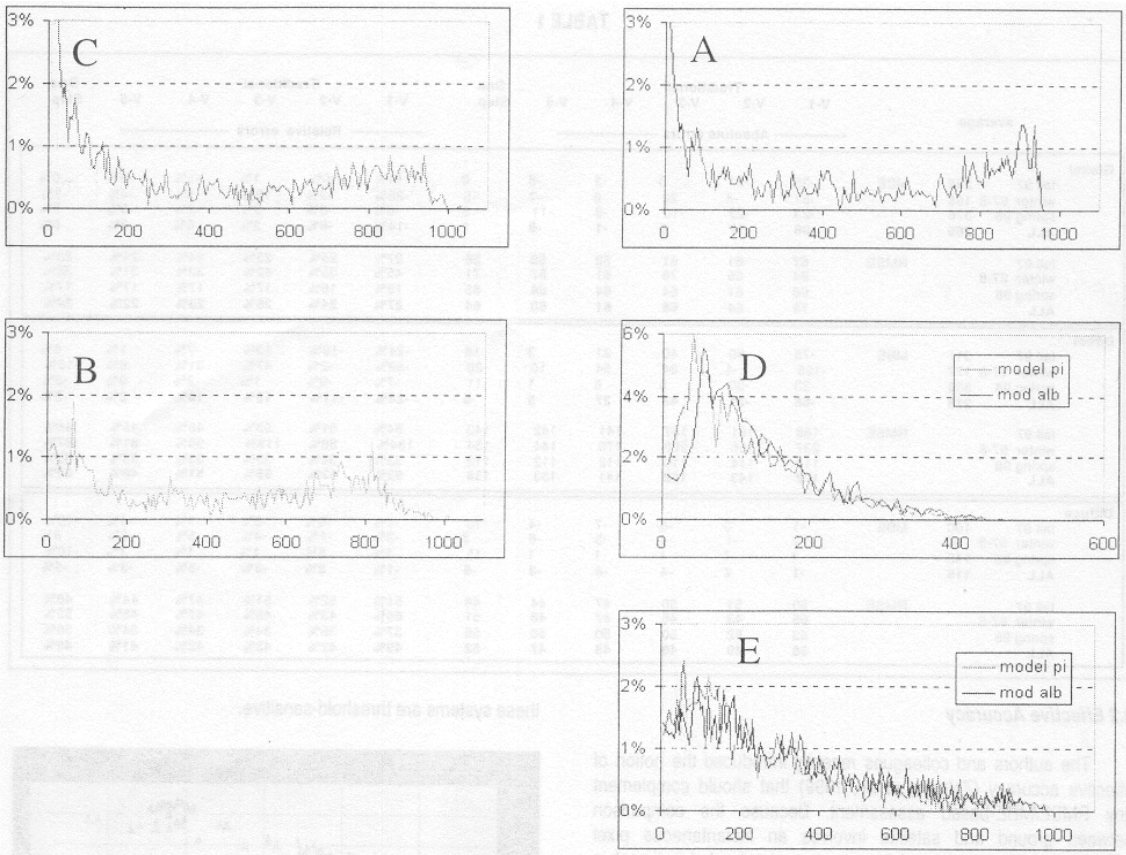

Figure 2: Ground (columns) and modeled (lines) frequency distributions for (a) the one-step direct model; (b) the version 1 traditional direct model; (c) the direct model obtained by difference of one-step global and one-step diffuse models; (d) the one-step and version 1 diffuse models; and (e) the one-step and version 1 global models.

4. CONCLUSIONS AND RECOMMENDATIONS

Our preliminary investigation in the one step modeling of direct and diffuse irradiance demonstrates substantial performance improvement potential. Follow-on work will be carried out for:

- Investigating and minimizing site-dependency by expanding the analysis to other climates/environments.
- Implementing effective albedo tracking in the one-step model, and making use of available external information.

We showed that the use of readily (or potentially) available, information consisting of cloud cover from meteorological services and regional turbidity resulted in measurable performance improvement, particularly in winter, at times of rapidly evolving ground albedos.

5. REFERENCE

Hammer, A., et al., 1998: Derivation of daylight and solar irradiance data from satellite observations. *9th Conf. on Satellite Meteorol. and Oceanography*, Amer. Meteor. Soc., Paris, 25th-29th May 1998, pp. 747-750.

Ineichen P. and R. Perez, 1999: Derivation of Cloud Index from Geostationary Satellites and Application to the Production of Solar Irradiance and Daylight Illuminance Data. *Theo. & Appl. Clim.* (in press -- accepted 6/99).

Kasten F., 1984: Parametrisierung der Globalstahlung durch Bedeckungsgrad und Trübungsfaktor. *Annalen der Meteorologie Neue Folge*, 20, 49-50.

Moussu, G., L. Diabaté, D. Obrecht and L. Wald, 1989: A method for the Mapping of the Apparent Ground Brightness Using Visible Images from Geostationary Satellites. *Int. J. Rem. Sensing*, 10-7, 1207-1225

Perez, R., P. Ineichen, E. Maxwell, R. Seals and A. Zelenka, 1992: Dynamic Global-to-Direct Irradiance Conversion Models. *ASHRAE Transactions-Research Series*, pp. 354-369

Schmetz, J. 1989: Towards a Surface Radiation Climatology -- Retrieval of Downward irradiances from Satellites. *Atmospheric Research*, 23, 287-231

Zelenka, A., R. Perez, R. Seals, and D. Renné, 1999: Effective Accuracy of Satellite-Derived Irradiance. *Theo. & Appl. Clim.* 62, 199-207.